



Title	Wideband Self-Interference Cancellation for 5G Full-Duplex Radio Using a Near-Field Sensor Array
Authors(s)	Keogh, Brian, Zhu, Anding
Publication date	2018-08-31
Publication information	Keogh, Brian, and Anding Zhu. "Wideband Self-Interference Cancellation for 5G Full-Duplex Radio Using a Near-Field Sensor Array." IEEE, August 31, 2018. https://doi.org/10.1109/IMWS-5G.2018.8484398 .
Conference details	2018 IEEE MTT-S International Microwave Workshop Series on 5G Hardware and System Technologies (IMWS-5G), University College Dublin, Ireland, 30-31 August 2018
Publisher	IEEE
Item record/more information	http://hdl.handle.net/10197/10538
Publisher's statement	© 2018 IEEE. Personal use of this material is permitted. Permission from IEEE must be obtained for all other uses, in any current or future media, including reprinting/republishing this material for advertising or promotional purposes, creating new collective works, for resale or redistribution to servers or lists, or reuse of any copyrighted component of this work in other works.
Publisher's version (DOI)	10.1109/IMWS-5G.2018.8484398

Downloaded 2026-05-02 00:30:28

The UCD community has made this article openly available. Please share how this access benefits you. Your story matters! (@ucd_oa)



© Some rights reserved. For more information

Wideband Self-Interference Cancellation for 5G Full-Duplex Radio Using a Near-Field Sensor Array

Brian Keogh^{*†} and Anding Zhu^{*}

^{*}School of Electrical and Electronic Engineering, University College Dublin, Ireland

[†]School of Engineering, Institute of Technology, Tallaght, Ireland

Email: brian.keogh.1@ucdconnect.ie

Abstract—Self-interference cancellation (SIC) is an important consideration for 5G wireless transceiver architectures. If successfully implemented, SIC can double spectral efficiency by allowing for in-band full-duplex operation. The main challenge lies in effective cancellation of the interference that is caused by the transmit signal. This paper presents a wide-band digitally controlled, analogue SIC circuit block employing a spatially adjustable near-field vector sensor. A stochastic perturbation algorithm operating in spatial and frequency domains provides efficient optimisation when used in combination with the hardware configuration. The proposed technique provides 35 dB of radio frequency suppression across a channel bandwidth of 100 MHz centred at 2.1 GHz.

Index terms — Self-interference cancellation, 5G radio architecture, Full-Duplex, RF FIR filter, SIC, SPSA.

I. INTRODUCTION

Future demands for higher mobile data rates poses a significant challenge for 5G radio front-end architectures, given that the RF spectrum is a limited public resource. Full-duplex transmission can address this problem because the up-link and down-link data streams simultaneously occupy the same spectrum allocation. Full-duplex operation is considered difficult to implement because the duplexer isolation between transmit and receive paths is not perfect. To address this problem, self-interference cancellation solutions typically combine propagation domain [1], RF domain [2], and digital domain cancellation [3]. The proposed cancellation technique is based on a single-antenna, RF SIC architecture as shown in Fig. 1. The isolation channel is comprised of the duplexer channel,

S_{31} , and channel reflections. The dominant interference signal is the known transmit signal (TX). The SIC design goal is to replicate, in anti-phase, the isolation channel S_{31} frequency domain response. In previous work by [4], the RF SIC circuit comprises fixed delay lines and programmable tap weights. An alternative circuit arrangement has recently been reported in [5] where an SIC circuit is placed on the antenna side of the duplexer. The key contribution in this paper is a novel technique to realise variable time delays, also on the antenna side, that can be controlled by an optimisation algorithm. The technique offers additional degrees of freedom for curve fitting in the frequency domain. A stochastic algorithm, based on [6], is used to optimise the delay lines in the spatial domain in addition to complex valued tap weights using frequency domain measurements. The paper is organised as follows: a hardware approach is described in Section II and an adaptive optimisation method is described in Section III. This is followed by a description of an RF vector sensor and SIC circuit implementation in Section IV. Section V concludes.

II. HARDWARE CONCEPT

To obtain an input for the SIC circuit, a TX coupler is usually used, as shown in Fig. 1. This TX coupler is interfaced to a splitter circuit in order to maintain 50Ω characteristic impedance on each delay line in the SIC circuit. The delays are typically implemented using either micro-strip or coaxial lines. This is expensive and restrictive because the delays are fixed. An alternative approach is shown in Fig. 2. The TX coupler, splitter and transmission lines are removed. Instead, copies of the TX signal are extracted using a near field sensor array as shown in Fig. 2. If the near-field sensors are attached to a programmable linear drive then the separation distances can be spatially optimised. The proposed sensor array therefore captures a set of time delayed copies of the actual transmitted pass-band signal, including TX signal impairments such as inter-modulation distortion and phase noise. The output of the SIC circuit shown in Fig. 2 is

$$\mathbf{Y} = \mathbf{W}_{a\phi} \mathbf{A}_\tau \mathbf{X}_{TX} \quad (1)$$

where \mathbf{Y} represents the frequency domain output matrix, \mathbf{A}_τ represents the spatial positioning of the near field sensors and $\mathbf{W}_{a\phi}$ represents the tap weights of the attenuators and phase shifters. \mathbf{X}_{TX} is comprised of discrete frequency samples,

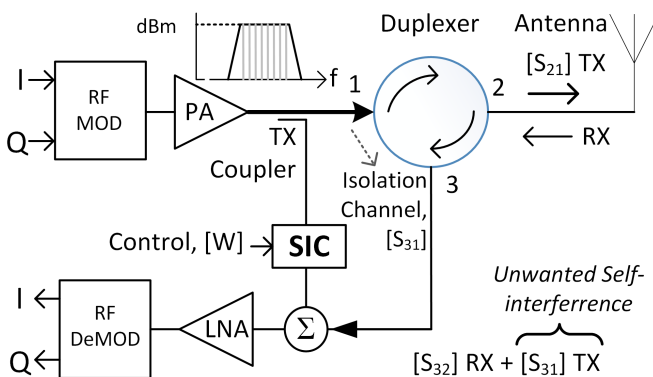


Fig. 1. Basic concept of RF self interference cancellation (SIC)

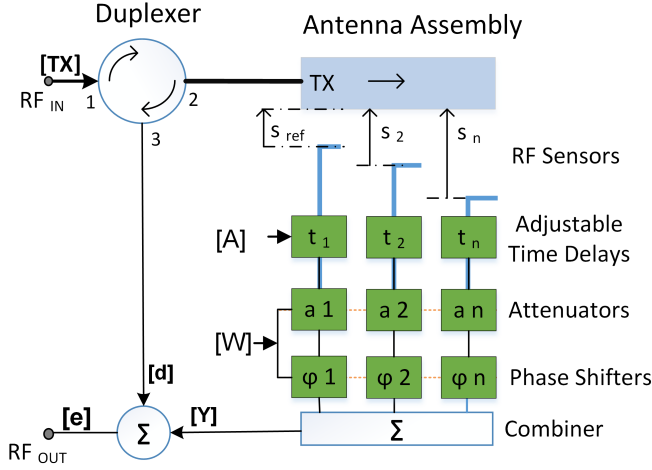


Fig. 2. Proposed hardware configuration

generated by a compact Vector Network Analyser. The output of the isolation channel at port 3 of the duplexer is given by

$$\mathbf{d} = \mathbf{S}_{31} \mathbf{X}_{TX} \quad (2)$$

The output of the combiner is

$$\mathbf{e} = \mathbf{S}_{32} \mathbf{R} + \mathbf{S}_{31} \mathbf{X}_{TX} + \mathbf{W}_{a\phi} \mathbf{A}_{\tau} \mathbf{X}_{TX} \quad (3)$$

where \mathbf{R} represents the receive signal. If \mathbf{R} is switched out during an initialisation phase and array \mathbf{e} is used as the input to an error function, then the frequency domain optimisation goal is that

$$\mathbf{W}_{a\phi} \mathbf{A}_{\tau} = -\mathbf{S}_{31} \quad (4)$$

Normalised mean square error (NMSE) is used to indicate closeness of fit across a selected bandwidth. As an illustrative

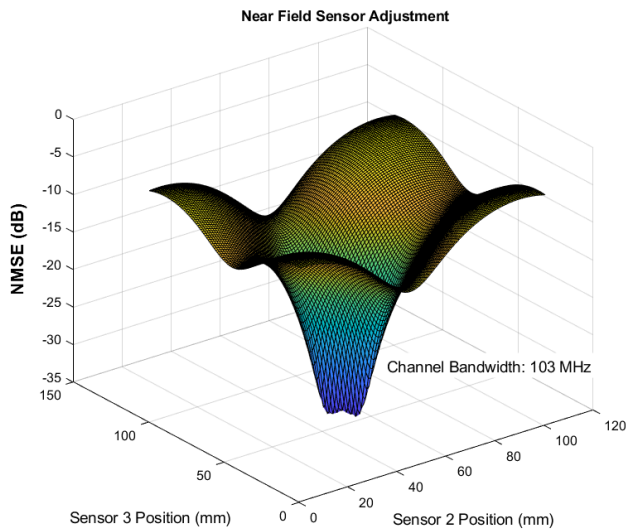


Fig. 3. NMSE result for the sensor with two degrees of movement

example, NMSE results for a sensor array with two degrees of freedom is shown in Fig. 3. A spatial adjustment of \mathbf{A}_{τ} will affect magnitude response. Therefore an optimisation algorithm should either simultaneously perturb all control inputs or preset the sensor array to a feasible position.

III. ADAPTIVE ALGORITHM

Each tap behaves as an RF vector modulator, comprised of a 6-bit attenuator and 6-bit phase shifter with 2^{12} constellation points per tap. An optimisation algorithm, *Simultaneous Perturbation Stochastic Approximation* (SPSA), [6], optimises SIC weights and spatial domain delays as shown in Fig. 4. The next iteration weight is based on the current weight minus a gradient estimate in each dimension and is given by

$$\hat{\Theta}_{k+1} = \hat{\Theta}_k - a_k \hat{g}_k(\hat{\Theta}_k) \quad (5)$$

where $\hat{\Theta}_k$ is the normalised weight vector, a_k is a weighting factor controlling the speed of convergence and $\hat{g}_k(\hat{\Theta}_k)$ represents the complex multidimensional gradient estimate of the objective function at $\hat{\Theta}_k$. The vector, $\hat{\Theta}_k$, comprises the attenuator and phase shifter settings for all taps. A strength of SPSA is that it uses measurement results of the objective function to approximate the gradient in each dimension instead of conducting direct differential calculation. In order to estimate the gradient, two additional vectors are generated by adding and subtracting a random perturbation sequence, Δ_k , to the existing vector, $\hat{\Theta}_k$, as follows

$$\begin{aligned} \hat{\Theta}_k^+ &= \hat{\Theta}_k + c_k \Delta_k \\ \hat{\Theta}_k^- &= \hat{\Theta}_k - c_k \Delta_k \end{aligned} \quad (6)$$

where c_k is a weighting factor. By applying the above coefficient vectors to the circuit, two measurements $L(\hat{\Theta}_k^+)$ and $L(\hat{\Theta}_k^-)$ are obtained. The gradient is estimated as

$$\hat{g}_k(\hat{\Theta}_k) = \frac{L(\hat{\Theta}_k^+) - L(\hat{\Theta}_k^-)}{\hat{\Theta}_k^+ - \hat{\Theta}_k^-} \quad (7)$$

A precise model of the SIC circuit and stepper motor drive assembly is not necessary since the only input to the algorithm is the NMSE result of each perturbation. Furthermore, no prior calibration of the stepper motor linear drive is required. As all

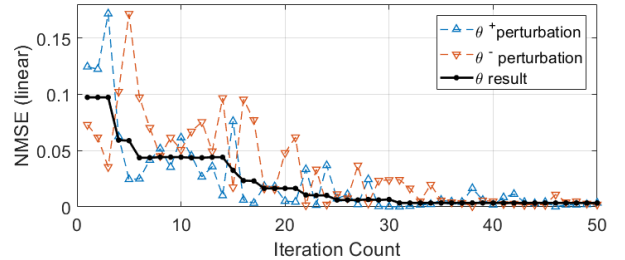


Fig. 4. SPSA convergence showing positive and negative perturbations

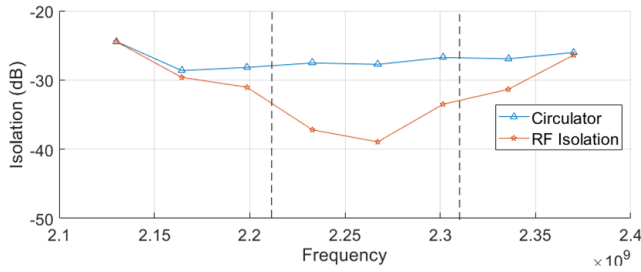


Fig. 5. RF isolation result over a 100MHz channel

elements of the coefficient vectors are perturbed simultaneously, the number of necessary measurements is independent from the number of coefficients, which reduces the complexity of calculation. Due to the non-ideal behaviour of RF hardware components and the discrete step size, the optimisation surface is irregular with local minima. The algorithm maintains a history of all NMSE results and can use this history as part of the weight update strategy.

IV. IMPLEMENTATION AND DISCUSSION

A 3-tap SIC is implemented on FR4 printed circuit board and is shown in Fig. 6. The phase shifters and attenuators are digitally controlled by a micro-controller unit over a serial peripheral interface. All RF paths and components in the SIC circuit are designed for a 50Ω characteristic impedance at a centre frequency of 2.1 GHz. The algorithm is designed to operate with hardware constraints such as limited non-linear attenuation step size, range limits, phase attenuation discontinuities and attenuator leakage. The frequency domain measurement system is based on a programmable compact vector network analyser as shown in Fig.7. A calibration routine is used to normalise all measurements with respect to fixed losses in the system. The RF isolation results in Fig. 5 show that this technique can offer an alternative way to recover time delayed copies of the TX signal.

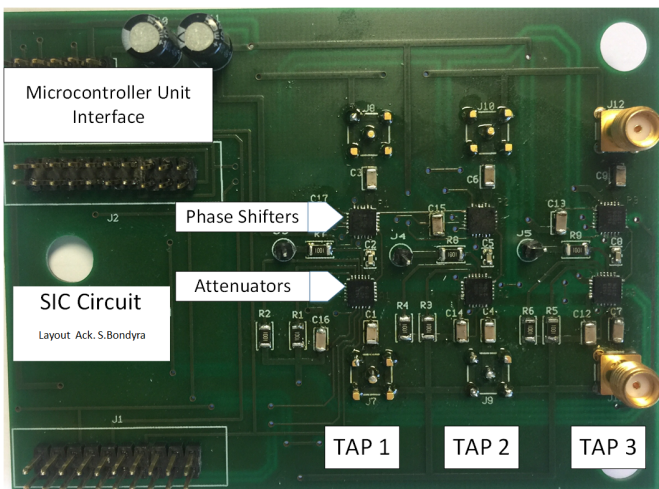


Fig. 6. Prototype of the SIC circuit

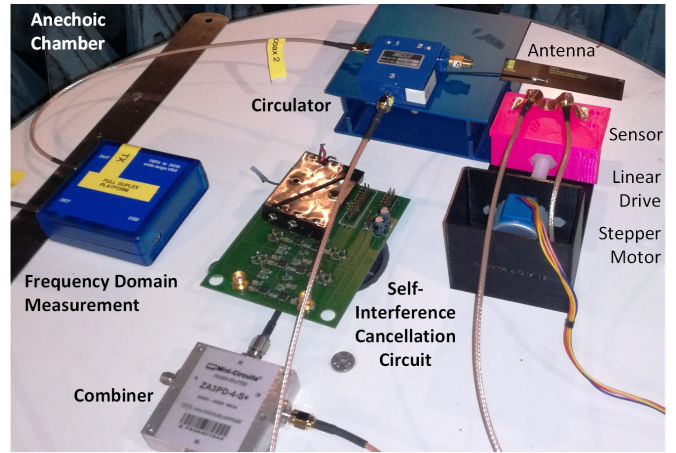


Fig. 7. System configuration using adjustable near field sensor

V. CONCLUSION

This paper has proposed a novel RF technique for self-cancellation using frequency domain and spatial domain optimisation. Evaluation of the RF hardware platform, when tested in an RF anechoic chamber, shows promising results for wide-band operation. The technique has applications for future 5G radio, in cases where a set of time delayed copies of the TX signal need to be monitored and used by an algorithm. The method obviates the need for a TX coupler, splitter and delay lines, with resulting savings in terms of cost and space. Finally, when combined with propagation domain and digital domain cancellation this work has applications for short-range line of sight 5G relay nodes or small cell back-haul in high spectral density environments.

ACKNOWLEDGEMENTS

This publication was emanated from research supported in part by research grants from Science Foundation Ireland (SFI) and co-funded under the European Regional Development Fund under Grant Numbers 13/RC/2077 and 12/IA/1267.

REFERENCES

- [1] M. Duarte, A. Sabharwal, V. Aggarwal, R. Jana, K. Ramakrishnan, C. W. Rice, and N. K. Shankaranarayanan, "Design and characterization of a full-duplex multi-antenna system for wifi networks," *IEEE Transactions on Vehicular Technology*, vol. 63, no. 3, pp. 1160–1177, March 2014.
- [2] U. S. Jha and F. Harris, "Spectral efficiency enhancements utilizing analog rf frontend in-band interference cancellation," in *2017 20th International Symposium on Wireless Personal Multimedia Communications (WPMC)*, Dec 2017, pp. 112–116.
- [3] S. Li and R. D. Murch, "An investigation into baseband techniques for single-channel full-duplex wireless communication systems," *IEEE Transactions on Wireless Communications*, vol. 13, no. 9, pp. 4794–4806, Sept 2014.
- [4] D. Bharadia, E. McMillin, and S. Katti, "Full duplex radios," *SIGCOMM Comput. Commun. Rev.*, vol. 43, no. 4, pp. 375–386, Aug. 2013. [Online]. Available: <http://doi.acm.org/10.1145/2534169.2486033>
- [5] S. Khaledian, F. Farzami, B. Smida, and D. Erricolo, "Inherent self-interference cancellation for in-band full-duplex single-antenna systems," *IEEE Transactions on Microwave Theory and Techniques*, pp. 1–9, 2018.
- [6] N. Kelly and A. Zhu, "A modified simultaneous perturbation stochastic optimization algorithm for digital predistortion model extraction," in *2015 Integrated Nonlinear Microwave and Millimetre-wave Circuits Workshop (INMMiC)*, Oct 2015, pp. 1–3.